

Radiative neutrino masses

Antonio Enrique Cárcamo Hernández

Departamento de Física, Universidad Técnica Federico Santa María
Centro Científico-Tecnológico de Valparaíso, Casilla 110-V, Valparaíso, Chile
Millennium Institute for Subatomic Physics at the High-Energy Frontier, SAPHIR, Chile

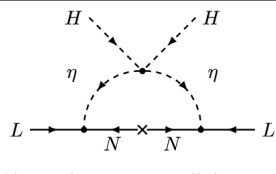
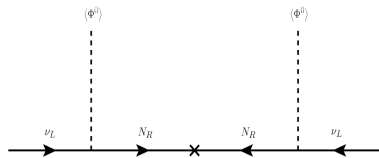
SUSY 2023 Conference, 21-07-2023.

Based on: C. Bonilla, AECH, B. Díaz Sáez, S. Kovalenko and

J. M. González, arxiv:hep-ph/2306.08453

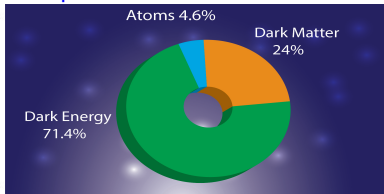
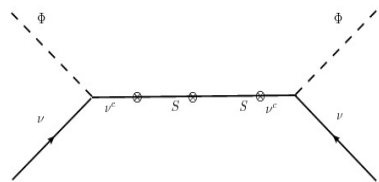
A. Abada, N. Bernal, AECH, S. Kovalenko, T. B. de Melo and
T. Toma, JHEP **03**, 035 (2023).

Introduction

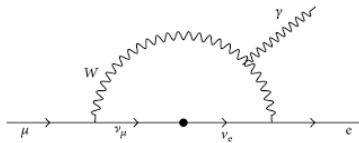


Type I seesaw mechanism

One loop Ma radiative seesaw model



Inverse seesaw mechanism

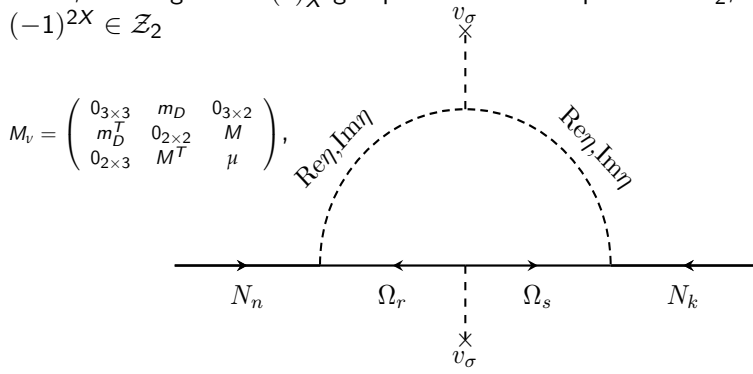


$$Br_{SM}(\mu \rightarrow e\gamma) \sim \mathcal{O}(10^{-54}), Br_{exp}(\mu \rightarrow e\gamma) < 4.2 \times 10^{-13}$$

Dark Matter from a Radiative Inverse Seesaw Model

	Φ	σ	η	L_{L_i}	I_{R_i}	ν_{R_k}	N_{R_k}	Ω_{R_k}
$SU(2)_L$	2	1	1	2	1	1	1	1
$U(1)_Y$	1/2	0	0	-1/2	-1	0	0	0
$U(1)_X$	0	-1	1/2	-1	-1	-1	1	-1/2

Table: Charge assignments of scalar and lepton fields. Here $i = 1, 2, 3$ and $k = 1, 2$. The global $U(1)_X$ group breaks down to preserved \mathbb{Z}_2 , with $(-1)^{2X} \in \mathbb{Z}_2$



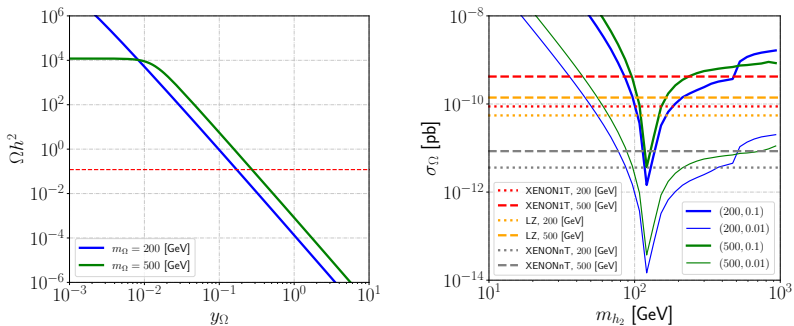


Figure: Left-panel: Relic abundance as a function of y_Ω for $m_\Omega = 200$ and 500 GeV. Here we have set $m_{h_2} = 120$ GeV and $\theta = 0.1$. Right-panel: Direct detection cross section as a function of m_{h_2} and different combinations of $(m_\Omega \text{ [GeV]}, \tan \theta)$. The horizontal red and orange lines are the current DD upper limits for each value of m_Ω , whereas the grey curves are the XENONnT projections. The solid curves depicted here fulfill the correct relic abundance.

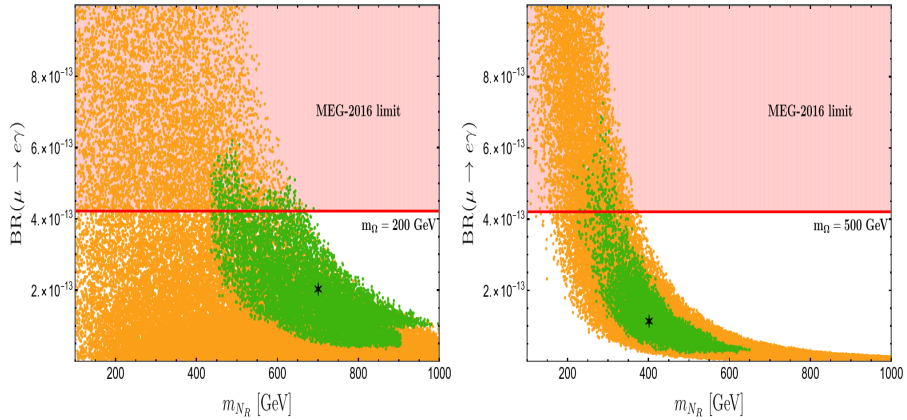
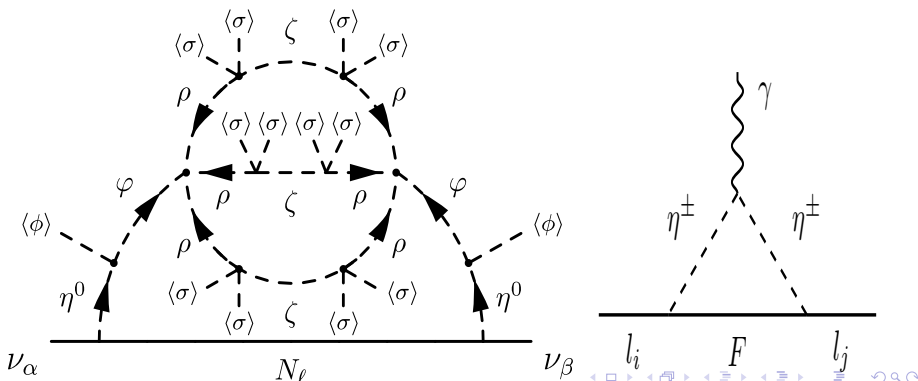


Figure: Branching ratio $\text{BR}(\mu \rightarrow e\gamma)$ as a function of the mass of the lightest RH Majorana neutrino N_R . The shadowed region is excluded by MEG. The black star corresponds to the prediction of the best-fit point of the model, for $m_\Omega = 200 \text{ GeV}$ (left-panel) and $m_\Omega = 500 \text{ GeV}$ (right-panel). The green points are compatible with current neutrino oscillation experimental limits at 3σ . The orange point are out of the 3σ range and, hence, excluded by neutrino oscillation data.

Scotogenic three-loop neutrino mass model

Field	q_{iL}	u_{iR}	d_{iR}	ℓ_{iL}	ℓ_{iR}	N_{R_k}	ϕ	η	φ	ρ	ζ	σ
$SU(3)_C$	3	3	3	1	1	1	1	1	1	1	1	1
$SU(2)_L$	2	1	1	2	1	1	2	2	1	1	1	1
$U(1)_Y$	$\frac{1}{6}$	$\frac{2}{3}$	$-\frac{1}{3}$	$-\frac{1}{2}$	-1	0	$\frac{1}{2}$	$\frac{1}{2}$	0	0	0	0
$U(1)'$	$\frac{1}{3}$	$\frac{1}{3}$	$\frac{1}{3}$	-3	-3	0	0	3	3	-1	0	$\frac{1}{2}$
\mathbb{Z}_2	1	1	1	1	1	-1	1	-1	-1	-1	-1	1

\mathbb{Z}_2 is preserved. The interaction $(\phi^\dagger \eta)^2$ arises at two-loop level.



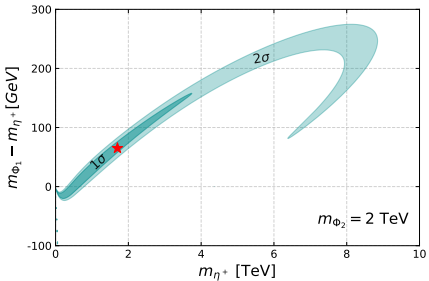
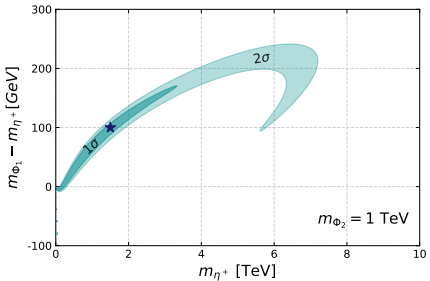
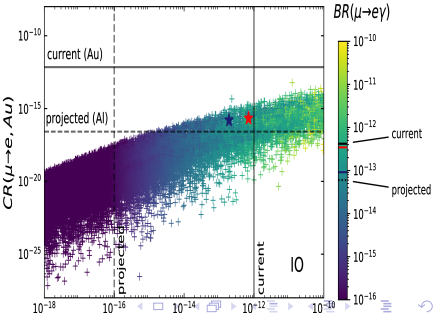
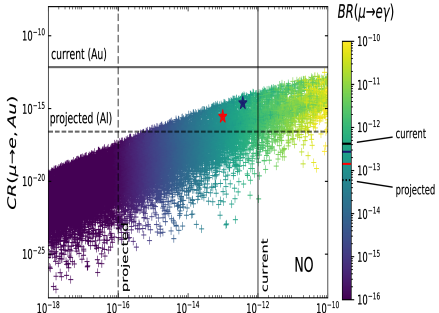
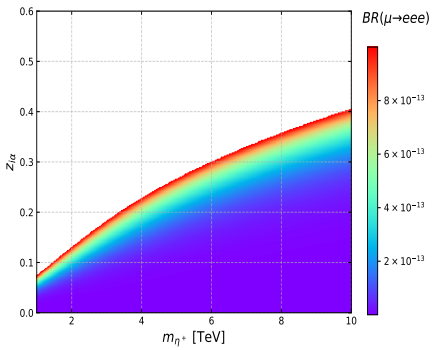
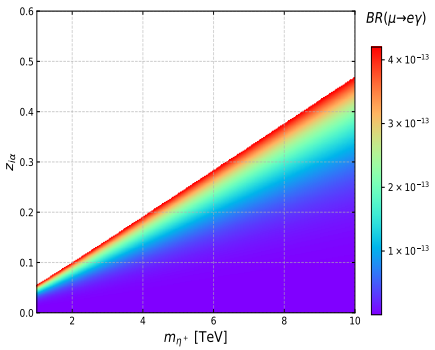


Figure: The 1σ and 2σ regions in the $m_{\Phi_1} - m_{\eta^+}$ versus m_{η^+} plane allowed by the fit of the oblique S , T and U parameters including the CDF measurement of the W mass. In the left (right) panel the mass of the neutral scalar Φ_2 is $m_{\Phi_2} = 1 \text{ TeV}$ ($m_{\Phi_2} = 2 \text{ TeV}$). In both cases, the mixing angle is fixed at $\theta_\Phi = 0.2$.



Conclusions

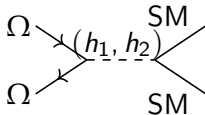
- Neutrino masses can be generated via radiative inverse seesaw.
- Dark matter stability can arise from a residual discrete symmetry.
- Dark matter and CLFV constraints can be accommodated in the Inverse Seesaw Majoron Model.
- 3-loop neutrino masses can appear in a minimally extended IDM.
- The minimal extended IDM accommodates oblique parameter constraints, W mass anomaly and leads to CLFV processes within the reach of the future experimental sensitivity.

Acknowledgements

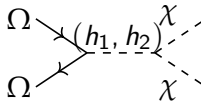
Thank you very much to all of you for the attention.

A.E.C.H was supported by Fondecyt (Chile), Grant No. 1210378,
Mileno-ANID-ICN2019 044 and ANID PIA/APOYO AFB220004.

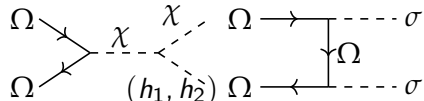
Extra Slides



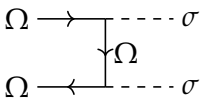
(a)



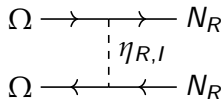
(b)



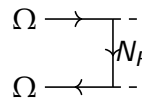
(c)



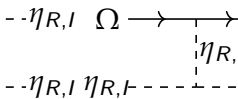
(d)



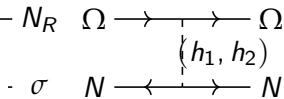
(e)



(f)



(g)



(h)

Figure: Diagrams (a)-(g) are relevant for the freeze-out of Ω . The diagram (h) is relevant for direct detection, with N representing the nucleons. Here to simplify notation we have used σ to denote either of (h_1, h_2, χ) .

Using the Casas–Ibarra parametrization

$$m_D = \frac{y_\nu v_\Phi}{\sqrt{2}} = U_{\text{PMNS}} (\hat{m}_\nu)^{1/2} \hat{R} \mu^{-1/2} M , \quad (1)$$

where $U_{\text{PMNS}} \equiv U_\ell^\dagger U_\nu$, $\hat{m}_\nu = \text{diag}(m_1, m_2, m_3)$ is the diagonal neutrino mass matrix and \hat{R} is a rotation matrix given by,

$$\hat{R} = \begin{pmatrix} 0 & 0 \\ \cos \hat{\theta} & \sin \hat{\theta} \\ -\sin \hat{\theta} & \cos \hat{\theta} \end{pmatrix} \quad \text{with } \hat{\theta} \in [0, 2\pi]. \quad (2)$$

We varied M_1 and y_B within the ranges $100 \text{ GeV} \leq M_1 \leq 1 \text{ TeV}$, $10^{-2} \leq y_N \leq 1$ and considered $M_2 = 10M_1$, $\mu_2 = 10\mu_1$. Furthermore, we fixed:

$$m_{\eta_R} = 2000 \text{ GeV}, \quad m_{\eta_I} = 2001 \text{ GeV}. \quad (3)$$

We also take the charged lepton mass matrix as a diagonal matrix, i.e. $M_l = \text{diag}(m_e, m_\mu, m_\tau)$, which implies $U_{\text{PMNS}} = U_\nu$ in Eq. (1).

Observable	$\Delta m_{21}^2 [10^{-5} \text{ eV}]$	$\Delta m_{31}^2 [10^{-3} \text{ eV}]$	$\sin^2 \theta_{12} / 10^{-1}$	$\sin^2 \theta_{23} / 10^{-1}$	$\sin^2 \theta_{13} / 10^{-2}$	$\delta_{CP} / {}^\circ$
Best fit $\pm 1\sigma$	$7.50^{+0.22}_{-0.20}$	$2.55^{+0.02}_{-0.03}$	3.18 ± 0.16	5.74 ± 0.14	$2.200^{+0.069}_{-0.062}$	194^{+24}_{-22}
3σ range	$6.94 - 8.14$	$2.47 - 2.63$	$2.71 - 3.69$	$4.34 - 6.10$	$2.00 - 2.405$	$128 - 359$

Observable	$\mu_1 [\text{keV}]$	$m_{N_R} [\text{GeV}]$	$\Delta m_{21}^2 [10^{-5} \text{eV}^2]$	$\Delta m_{31}^2 [10^{-3} \text{eV}^2]$	$\sin \theta_{12}^{(I)} / 10^{-1}$	$\sin \theta_{13}^{(I)} / 10^{-3}$	$\sin \theta_{23}^{(I)} / 10^{-1}$	$\delta_{CP}^{(I)} ({}^\circ)$
Best fit case (a)	-0.562	700.5	7.53	2.51	3.53	2.11	5.66	195.3
Best fit case (b)	-0.4099	401.3	7.50	2.55	3.25	2.22	5.64	174.8

Table: Best fit values of the model. Case (a) considers $m_\Omega = 200$ GeV and case (b) is for $m_\Omega = 500$ GeV.

Dimensionless parameters (a)	
$y_{\nu_{11}} = 0.0109 e^{1.87i}$	$y_{\nu_{31}} = 0.0124 e^{1.49i}$
$y_{\nu_{12}} = 0.0105 e^{-1.31i}$	$y_{\nu_{32}} = 0.0808 e^{1.77i}$
$y_{\nu_{21}} = 0.0270 e^{1.70i}$	$y_N = 2.04 \times 10^{-2}$
$y_{\nu_{22}} = 0.0463 e^{1.56i}$	$\hat{\theta} = 1.303 \text{ rad}$

Dimensionless parameters (b)	
$y_{\nu_{11}} = 0.00525 e^{-1.51i}$	$y_{\nu_{31}} = 0.0177 e^{1.572i}$
$y_{\nu_{12}} = 0.0151 e^{-1.59i}$	$y_{\nu_{32}} = 0.00424 e^{1.61i}$
$y_{\nu_{21}} = 0.0166 e^{1.57i}$	$y_N = 1.22 \times 10^{-2}$
$y_{\nu_{22}} = 0.0354 e^{-1.58i}$	$\hat{\theta} = -4.98 \text{ rad}$

$$\begin{pmatrix} \eta^0 \\ \varphi \end{pmatrix} = \begin{pmatrix} \cos \theta_\Phi & \sin \theta_\Phi \\ -\sin \theta_\Phi & \cos \theta_\Phi \end{pmatrix} \begin{pmatrix} \Phi_1 \\ \Phi_2 \end{pmatrix}, \quad (4)$$

$$\begin{pmatrix} \rho_R \\ \zeta_R \end{pmatrix} = \begin{pmatrix} \cos \theta_\Xi & \sin \theta_\Xi \\ -\sin \theta_\Xi & \cos \theta_\Xi \end{pmatrix} \begin{pmatrix} \Xi_1 \\ \Xi_2 \end{pmatrix}, \quad (5)$$

$$\begin{pmatrix} \rho_I \\ \zeta_I \end{pmatrix} = \begin{pmatrix} \cos \theta'_\Xi & \sin \theta'_\Xi \\ -\sin \theta'_\Xi & \cos \theta'_\Xi \end{pmatrix} \begin{pmatrix} \Xi_3 \\ \Xi_4 \end{pmatrix}. \quad (6)$$

Parameters	Scanned ranges
θ_R	$[0, 2\pi]$
λ_{14}	$[0.01, 1]$
$m_{N_R}, m_{\eta^+}, m_{\Phi_{1,2}}, m_{\Xi_{1,2,3,4}}$	$[500, 10000]$ GeV

Table: Scanned parameter ranges.

θ_Φ	0.2	0.2
θ_Ξ	0.3	0.3
θ'_Ξ	0.1	0.1
m_{η^+} [GeV]	1500	1700
m_{Φ_1} [GeV]	1600	1765
m_{Φ_2} [GeV]	1000	2000
m_{N_R} [GeV]	8954.5	4246.9
m_{Ξ_1} [GeV]	8130.4	2925.0
m_{Ξ_2} [GeV]	1452.5	4748.5
m_{Ξ_3} [GeV]	8932.4	2763.1
m_{Ξ_4} [GeV]	7127.2	9336.4
λ_{14}	0.729	0.726
y_η^{e1}	0.124	0.346
y_η^{e2}	-0.253	0.389
$y_\eta^{\mu 1}$	0.746	0.220
$y_\eta^{\mu 2}$	-0.307	-0.272
$y_\eta^{\tau 1}$	0.705	-0.335
$y_\eta^{\tau 2}$	0.207	0.225
$\text{BR}(\mu \rightarrow e\gamma)$	2.730×10^{-13}	9.170×10^{-14}
$\text{BR}(\mu \rightarrow eee)$	3.686×10^{-13}	1.933×10^{-13}
$\text{BR}(\mu - e, Au)$	2.392×10^{-15}	1.599×10^{-16}
m_{ee} [meV]	3.67	48.36
	3.67	48.36

The one-loop contributions to the oblique parameters T , S and U are defined as:

$$T = \frac{\Pi_{33}(q^2) - \Pi_{11}(q^2)}{\alpha_{EM}(M_Z) M_W^2} \Big|_{q^2=0}, \quad S = \frac{2 \sin 2\theta_W}{\alpha_{EM}(M_Z)} \frac{d\Pi_{30}(q^2)}{dq^2} \Big|_{q^2=0},$$
$$U = \frac{4 \sin^2 \theta_W}{\alpha_{EM}(M_Z)} \left(\frac{d\Pi_{33}(q^2)}{dq^2} - \frac{d\Pi_{11}(q^2)}{dq^2} \right) \Big|_{q^2=0}$$

where $\Pi_{11}(0)$, $\Pi_{33}(0)$, and $\Pi_{30}(q^2)$ are the vacuum polarization amplitudes with $\{W_\mu^1, W_\mu^1\}$, $\{W_\mu^3, W_\mu^3\}$ and $\{W_\mu^3, B_\mu\}$ external gauge bosons, respectively, and q is their momentum. The experimental values of T , S and U before the CDF measurement are:

$$T = -0.01 \pm 0.10, \quad S = 0.03 \pm 0.12, \quad U = 0.02 \pm 0.11. \quad (7)$$

After the CDF measurement:

$$T = 0.11 \pm 0.12, \quad S = 0.06 \pm 0.10, \quad U = 0.14 \pm 0.09. \quad (8)$$